

Regular article

Vibrational linestrengths for the ground and first excited electronic states of HeH_2^+

M. Šindelka^{1,2}, V. Špirko^{1,2}, W. P. Kraemer²

¹ J. Heyrovský Institute of Physical Chemistry, Academy of Sciences of the Czech Republic and Center for Complex Molecular Systems and Biomolecules, Dolejškova 3, 182 23 Prague 8, Czech Republic

² Max-Planck Institute of Astrophysics, Postfach 1317, 85741 Garching, Germany

Received: 10 April 2002 / Accepted: 24 September 2002 / Published online: 7 October 2003
© Springer-Verlag 2003

Abstract. Together with recent improved potential-energy surface calculations for the ground (\tilde{X}) and first excited (\tilde{A}) electronic states of HeH_2^+ , the electric dipole moment surfaces for each state and the transition dipole moments connecting the two states were evaluated for the entire range of the energy calculations. Using these functions the linestrengths of all dipole-allowed transitions between the bound vibrational levels within each of the two states ($\tilde{X} \rightarrow \tilde{X}$) and ($\tilde{A} \rightarrow \tilde{A}$) as well as between them ($\tilde{A} \rightarrow \tilde{X}$) are evaluated here. These data are believed to be useful both in the experimental search for the yet unobserved molecular spectra of HeH_2^+ and in evaluating theoretical rates for the radiative association or photodissociation processes involving the two lowest electronic states of the ion.

Keywords: Vibrational line strength – HeH_2^+ – Electric dipole moment surface – Transition dipole moment

1 Introduction

Since hydrogen and helium are the two most abundant elements in most interstellar environments, collisional interactions between their atomic (H , H^+ , He , He^+) or molecular (H_2 , H_2^+) forms are considered to be of possible astrophysical importance [1]. Among these the radiative charge-transfer reaction



is of major interest and has previously been studied in the laboratory [2].

A complete quantum mechanical state-to-state description of this process requires knowledge of the potential-energy and electric dipole moment functions of

the ground \tilde{X} and first excited \tilde{A} electronic states of the HeH_2^+ complex together with the transition dipole moment function connecting the two states (each of these functions extending over the entire range of the collisional configurations) and the evaluation of the corresponding ro-vibrational wavefunctions and dipole moment matrix elements.

The present paper describes the calculation of these functions and of the dipole-allowed bound-bound transitions. The calculations use recently published ab initio results for the potential-energy functions of the ground and first excited electronic states [3] and simultaneously calculated electric dipole moment and transition dipole moment data. Details of the ab initio calculations were described previously [3]. The ground-state potential presented in Ref. [3] agrees very well with two other recently improved potential function calculations [4, 5].

The present calculations are done in analogy to earlier ground-state studies [6, 7] which were based on an older, less accurate set of ab initio data [8].

2 Electric dipole moment surfaces

Jacobi coordinates are used here, with r denoting the HH distance, R the distance between the He atom and the HH center of mass, and θ the angle between the \mathbf{r} and \mathbf{R} vectors. In both electronic states the ion is oriented in the body-fixed coordinate system such that it is placed in the (x, y) plane with the z -axis embedded along \mathbf{R} and with the origin of the coordinate system at the center of mass. In this reference configuration there is only one nonzero dipole moment component, which is expressed here as

$$\mu_z(r, R, \theta) = B \frac{m_{\text{He}}}{m_{\text{He}} + 2m_{\text{H}}} R + \sum_{k,l,m} C^z(k, l, m) [r \exp[-a_{rz}r]]^k [R \exp[-a_{Rz}R]]^l P_m(\cos \theta) \quad (2)$$

In this expression $B(\tilde{X}) = -1$, $B(\tilde{A}) = 1$, and $B(\tilde{X} \rightarrow \tilde{A}) = 0$, whereas $C^z(k, l, m)$, a_{rz} and a_{Rz} are “free”

Contribution to the Björn Roos Honorary Issue

Correspondence to: W.P. Kraemer
e-mail: wpk@mpa-garching.mpg.de

parameters, P_m are Legendre polynomials, and m_{He} , m_{H} are the corresponding atomic masses. In the two-step fitting procedure initially the nonlinear parameters a_{rz} and a_{Rz} are optimized to achieve optimum flexibility of the fitting functions, and then after fixing them at their optimized values the other parameters are determined by linear fits. The μ_z components of the pure dipole moments of the two states are asymptotically linear in R . Only ten parameters are needed to fit them and the standard deviations of the fits are 0.00639 and 0.00495 au, respectively. The asymptotically vanishing z component of the transition dipole moment is fitted using only nine parameters with a standard deviation of 0.00134 au. The results of the three fits are collected in Table 1. The stretching coordinates are assumed to be in angstroms and multiplication of the values resulting from Eq.(2) by 2.541766/0.529177 gives the dipole moments in debyes.

3 Results and discussion

The calculations were performed without introducing the Eckart frame because the equilibrium structures of the two electronic states are completely different and the main interest is in the transition processes between the two states. The formalism of the Sutcliffe–Tennyson Hamiltonian for triatomic molecules [9] was adapted in

the calculations. Rather than applying a variational solution of the eigenvalue problem as previously [3, 8], a coupled-channel approach is used here. For this purpose basis functions for the high-frequency HH stretch and the bending motion are first obtained numerically from the corresponding uncoupled one-dimensional Schrödinger equations and the common basis in r and θ is then constructed as a direct product of these one-dimensional bases. With this basis the three-dimensional eigenproblem is transformed into a system of coupled second-order differential equations containing only the “dissociation coordinate” R as an independent variable. Solution of this system is achieved numerically using the renormalized Numerov method of Johnson [10]. The bound vibrational energies for the two electronic states calculated by this approach are listed in Table 2. Here and in the following discussion the previously used labeling scheme for the vibrational levels is applied, i.e. v_r denotes the vibrational quantum number for the high-frequency HH stretch, whereas v_s and v_b are used to label the low-frequency stretching and bending modes, respectively. The energies for the ground electronic state in Table 2 are in close agreement with the corresponding results obtained recently from another ground-state potential calculation aiming at high accuracy [5]. This underlines the confidence which can be put into the ab initio data used in this study. Since potential energies for

Table 1. Electric dipole and transition dipole moment function parameters of HeH_2^+

i	j	k	$C_{ijk}^z(\tilde{\text{X}})^a$	i	j	k	$C_{ijk}^z(\tilde{\text{A}})^b$	i	j	k	$C_{ijk}^z(\tilde{\text{X}} \rightarrow \tilde{\text{A}})^c$
0	1	0	0.29945	1	1	0	-0.54346	1	1	0	-1.06396
1	3	0	-20.85718	0	2	0	-1.90571	0	2	0	23.12198
0	4	0	46.78664	2	1	0	-0.74780	2	1	0	1.11638
2	3	0	14.84419	1	2	0	5.72736	1	2	0	-8.38943
0	2	2	6.20984	0	4	0	-77.48615	0	3	0	-44.27047
1	2	2	-12.85417	0	5	0	180.29549	0	2	2	6.77757
0	3	2	-18.16457	3	1	2	-0.31926	1	2	2	-4.13108
2	2	2	5.73729	1	3	2	-7.54442	0	3	2	-17.70227
1	3	2	29.73729	2	3	2	6.46307	5	1	2	0.22999
2	2	4	0.19467	0	5	2	24.44867				

^a $a_{rz} = 0.025$, $a_{Rz} = 1.173$

^b $a_{rz} = 0.025$, $a_{Rz} = 0.985$

^c $a_{rz} = 0.025$, $a_{Rz} = 1.202$

Table 2. Bound vibrational energy levels of the electronic ground ($\tilde{\text{X}}$) and excited ($\tilde{\text{A}}$) states of $^4\text{HeH}_2^+$ (cm^{-1}). The numbers in *parentheses* give the differences of the vibrational energies obtained by the Born–Oppenheimer approximation from the full-dimensional results

$s_i^{(a)}$	v_s	v_b	E_{vib}	v_s	v_b	E_{vib}	v_s	v_b	E_{vib}	v_s	v_b	E_{vib}
	$\tilde{\text{X}}$ state			$\tilde{\text{A}}$ state ^(b)								
	j even			j odd			j even			j odd		
1	0	0	0.0 ^c (-5.6)	0	0	0.0 ^d (-5.6)	0	0	0.0 ^e (1.0)	0	0	426.6 (2.4)
2	1	0	726.2 (8.2)	1	0	726.3 (8.1)	1	0	278.6 (-0.1)	1	0	649.1 (0.1)
3	0	2	1131.1 (-2.1)	0	2	1133.2 (-5.9)	2	0	490.7 (-0.5)	2	0	803.6 (-0.7)
4	2	0	1245.4 (22.2)	2	0	1246.1 (21.2)	3	0	639.8 (-0.5)			
5	3	0	1480.9 (-41.3)	3	0	1526.9 (-19.2)	4	0	733.8 (-0.4)			
6	1	2	1564.3 (30.7)	1	2	1590.9 (4.9)	0	2	761.6 (3.2)			
7	4	0	1665.6 (6.0)	4	0	1725.0 (2.0)	5	0	785.1 (-0.2)			
8	5	0	1712.4 (25.0)				6	0	807.9 (-0.1)			
9	1	4	1752.6 (17.1)				7	0	816.0			

^a Formal labeling of the vibrational states

^b Dissociation limit of the $\tilde{\text{A}}$ state lying 73476 cm^{-1} above the dissociation limit of the $\tilde{\text{X}}$ state

^c Lying 1763.6 cm^{-1} below the dissociation limit

^d Lying 0.0007 cm^{-1} above the vibrational (j -even) ground state

^e Lying 817.5 cm^{-1} below the dissociation limit

both electronic states were calculated on the same accuracy level it can be assumed that the energies in Table 2 for the excited \tilde{A} state are also equally reliable.

Apart from solving the nuclear Schrödinger equations directly for the full-dimensional Sutcliffe–Tennyson Hamiltonian, an adiabatic separation of the nuclear motions with different energy contents is also applied here in analogy to the concept of the Born–Oppenheimer approximation for electronic and nuclear motions. For this purpose the total vibrational wavefunction is factorized according to

$$\Psi(r, R, \theta) = \psi(r, \theta; R)\Phi(R) \quad , \quad (4)$$

separating thus the high-frequency HH stretch and bending modes from the “dissociation motion”. Different factorizations were previously used for the HeH_2^+ ion [3, 8]. It has already been discussed [3] that these adiabatic separation schemes usually work perfectly well for weakly interacting systems, such as the excited \tilde{A} state in the present case, whereas for the more strongly bound ground state the reliability was found to be less satisfactory especially when going to higher vibrational levels. This is also shown in Table 2, where the numbers

in parentheses give the displacements of the Born–Oppenheimer approximated vibrational energies from the corresponding full-dimensional results. In contrast to the close agreement for the excited \tilde{A} state, fairly large differences are obtained between these two approaches for the ground electronic state. For this state the number of bound j -even levels also differs.

The results of the vibrational linestrength calculations for transitions between the bound vibrational levels in each of the two electronic states are listed in Tables 3 and 4, respectively. Each table is organized in rectangular form with the linestrength data derived from the full-dimensional variational calculations in the upper triangle, whereas the results obtained within the adiabatic Born–Oppenheimer separation are in parentheses in the lower triangle.

The agreement of the present linestrength results for the \tilde{X} state transitions listed in the upper triangle of Table 3 with the j -even state results of our earlier calculation [8] is fairly reasonable. This shows that the previously predicted spectral characteristics [6, 7] are essentially correct. Comparison however between the upper and lower triangles in Table 3 indicates that the

Table 3. Vibrational linestrengths, $S_{s_1 \leftrightarrow s_2}$, of transitions between bound vibrational levels in the ground electronic state of HeH_2^+ (10^{-4} debye²). The values in the upper triangle are derived from full-

dimensional calculations, whereas the corresponding values in the lower triangle (in *parentheses*) are obtained using the adiabatic Born–Oppenheimer separation scheme of Eq. (4)

$s_1 / s_2^{(a)}$	1	2	3	4	5	6	7	8	9
	<i>j</i> even								
1	14.138 (14.05)	0.465	0.001	0.052	0.000	0.011	0.000	0.004	0.001
2	(0.468)	21.381 (21.11)	0.161	0.701	0.060	0.059	0.032	0.001	0.004
3	(0.032)	(0.000)	19.539 (19.22)	0.184	0.460	0.025	0.116	0.081	0.008
4	(0.035)	(0.899)	(0.000)	31.503 (32.21)	0.197	0.819	0.186	0.020	0.034
5	(0.004)	(0.007)	(0.569)	(0.000)	39.562 (36.92)	0.380	0.897	0.185	0.001
6	(0.005)	(0.119)	(0.000)	(1.189)	(0.000)	49.463 (52.31)	0.368	0.734	0.249
7	(0.041)	(0.002)	(0.031)	(0.000)	(0.000)	(0.000)	63.027 (21.98)	2.239	0.022
8	(0.001)	(0.028)	(0.000)	(0.203)	(0.000)	(1.418)	(0.000)	84.636 (92.39)	3.418
9	(0.001)	(0.004)	(0.119)	(0.001)	(1.140)	(0.000)	(0.000)	(0.000)	202.15 (55.34)
	<i>j</i> odd								
1	14.137 (14.05)	0.464	0.002	0.052	0.001	0.012	0.001		
2	(0.468)	21.377 (21.10)	0.161	0.707	0.098	0.027	0.031		
3	(0.020)	(0.007)	19.316 (18.75)	0.175	0.440	0.186	0.009		
4	(0.035)	(0.902)	(0.000)	31.415 (31.98)	0.561	0.521	0.219		
5	(0.005)	(0.122)	(0.001)	(1.226)	40.488 (49.97)	0.727	0.723		
6	(0.010)	(0.000)	(0.578)	(0.003)	(0.000)	40.774 (31.86)	0.811		
7	(0.000)	(0.030)	(0.000)	(0.211)	(1.473)	(0.000)	79.984 (83.34)		

^a Labels s_i ($i = 1, 2$) refer to the formal labeling in Table 2

Table 4. Vibrational linestrengths, $S_{s_1 \leftrightarrow s_2}$, of transitions between bound vibrational levels of the first excited electronic state of HeH_2^+ (10^{-4} debye²). The values in the upper triangle are derived from full-

dimensional calculations, whereas the corresponding values in the lower triangle (in *parentheses*) are obtained using the adiabatic Born-Oppenheimer separation scheme of Eq. (4)

$s_1/s_2^{(a)}$	1	2	3	4	5	6	7	8	9
	<i>j</i> even								
1	55.185 (55.16)	0.527	0.032	0.005	0.001	0.005	0.000	0.000	0.000
2	(0.529)	68.059 (68.11)	1.125	0.111	0.024	0.001	0.007	0.002	0.001
3	(0.033)	(1.128)	87.251 (87.39)	1.813	0.240	0.000	0.062	0.018	0.005
4	(0.005)	(0.113)	(1.814)	118.14 (118.4)	2.651	0.000	0.402	0.103	0.025
5	(0.001)	(0.025)	(0.241)	(2.651)	172.13 (172.7)	0.011	3.794	0.585	0.125
6	(0.001)	(0.000)	(0.000)	(0.000)	(0.000)	67.685 (67.33)	0.014	0.000	0.000
7	(0.000)	(0.008)	(0.062)	(0.402)	(3.801)	(0.000)	278.34 (279.5)	5.869	0.782
8	(0.000)	(0.002)	(0.018)	(0.103)	(0.585)	(0.000)	(5.879)	521.97 (524.5)	10.354
9	(0.000)	(0.001)	(0.005)	(0.025)	(0.125)	(0.000)	(0.779)	(10.37)	1267.8 (1279.)
	<i>j</i> odd								
1	61.640 (61.51)	0.616	0.042						
2	(0.620)	78.802 (78.98)	1.346						
3	(0.046)	(1.341)	108.78 (109.3)						

(a) Labels s_i ($i = 1, 2$) refer to the formal labeling in Table 2

Table 5. Vibrational line-strengths, $\langle s_1(\tilde{\mathbf{X}}) | \mu_z^{\tilde{\mathbf{X}} \leftrightarrow \tilde{\mathbf{A}}} | s_2(\tilde{\mathbf{A}}) \rangle^2$, of transitions between bound vibrational levels of the ground and first excited electronic states of HeH_2^+ (10^{-4} debye²)

No. ^a	$s_1(\tilde{\mathbf{X}})/s_2(\tilde{\mathbf{A}})^b$	1	2	3	4	5	6	7	8	9
		<i>j</i> even								
(1–9)	1	0.01	0.01	0.01	0.00	0.01	0.00	0.00	0.00	0.00
(10–18)	2	0.74	0.63	0.41	0.24	0.14	1.50	0.05	0.02	0.01
(19–27)	3	6.57	4.85	3.28	2.06	1.21	4.14	0.51	0.20	0.06
(28–36)	4	18.60	3.90	0.92	0.24	0.11	38.58	0.00	0.00	0.00
(37–45)	5	217.20	55.75	32.52	18.39	10.18	28.46	4.22	1.66	0.46
(46–54)	6	3.47	59.95	28.72	17.10	8.46	108.75	4.99	1.78	0.49
(55–63)	7	88.67	5.81	4.35	0.65	0.22	19.35	0.16	0.05	0.01
(64–72)	8	86.64	36.59	2.71	0.15	0.01	10.62	0.00	0.00	0.00
(73–81)	9	8.88	19.72	0.81	0.51	0.03	3.29	0.01	0.00	0.00
		<i>j</i> odd								
	1	0.01	0.02	0.02	0.01					
	2	1.57	1.78	1.25	0.63					
	3	6.52	6.01	3.94	1.96					
	4	39.12	20.05	8.26	2.98					
	5	174.18	34.76	12.10	4.45					
	6	19.94	17.90	21.33	13.08					
	7	16.90	50.14	0.64	0.01					
	8	32.76	5.01	3.75	0.01					
	9	19.81	24.45	3.87	0.20					

^a Formal labeling of the *j*-even transitions for the stick diagram in Fig. 1

^b Labels s_i ($i = 1, 2$) refer to the formal labeling in Table 2

adiabatic approximation based on Eq. (4) is rather poor in this case.

As stated before, the approximation performs much better when applied to the weakly bound $\tilde{\mathbf{A}}$ state of the HeH_2^+ ion. Comparison of the upper and lower triangles in Table 4 gives good agreement between most of the entries. There is practically quantitative matching of the linestrength results for the van der Waals like stretching states, and also a rather close correspondence between

the linestrengths of transitions in which bending states are involved. From this result it can be concluded that dissociation or association processes taking place only on the $\tilde{\mathbf{A}}$ state potential-energy surface can conveniently be treated using simple one-dimensional modeling schemes.

The linestrength results obtained from full-dimensional calculations are collected in Table 5 for transitions between bound vibrational levels in different electronic

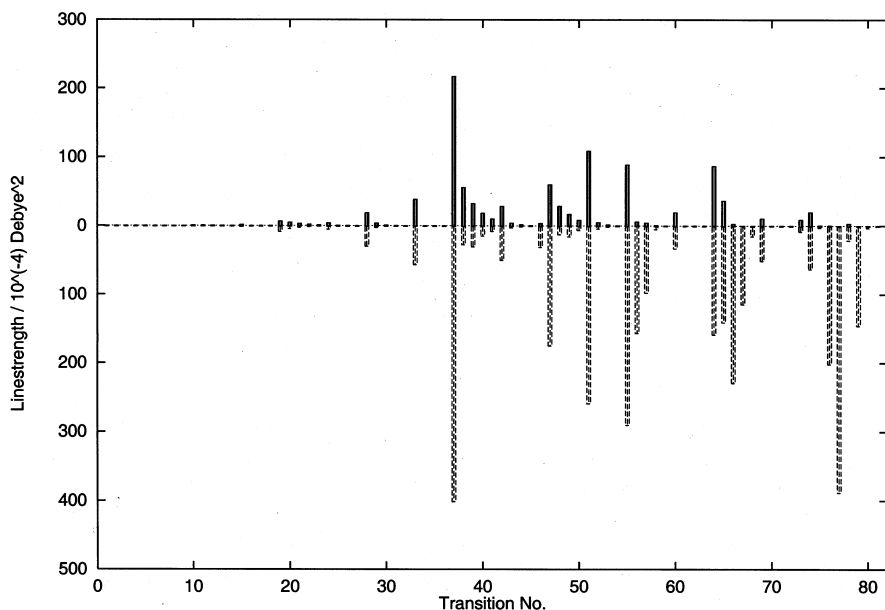


Fig. 1. Comparison of the linestrengths obtained from full-dimensional calculations (*solid lines* in the *upper part* of the plot) with Franck-Condon factors (*dashed lines* in the *lower part* of the plot) for transitions between the bound j -even vibrational levels of the ground (\tilde{X}) and first excited (\tilde{A}) electronic states of HeH_2^+

states ($\tilde{X} \rightarrow \tilde{A}$). Comparisons are made in the figures to see to which extent these results can be reproduced by simpler approximations. The stick diagrams in the upper and lower parts of Fig. 1 show the full-dimensional linestrength results for the transitions between bound j -even states together with the corresponding Franck-Condon factors. For all the transitions the Franck-Condon factors turn out to be much larger than the exact linestrengths and the overall patterns of the two stick diagrams are quite different. This makes it clear that non-Franck-Condon effects cannot be neglected at any physically meaningful theory level in this case. A comparison with the results derived from calculations using the Born-Oppenheimer approximation is made in Fig. 2. Since for the \tilde{X} electronic state the number of the j -even bound levels is different for the two approaches,

the j -odd transitions are used in this comparison. The differences are again substantial. Only for the lower 20 transitions are the general patterns of the two diagrams similar. From the plots it can therefore be concluded that a rather reliable theory level is required for a sufficiently accurate description of the two electronic states which have very different bond characteristics.

Summarizing the results of this study it is shown here that the newly available improved ab initio data [3] provide a reliable basis for studying the two lowest electronic states of the HeH_2^+ ion. The new results for the ground electronic state agree closely with other high-accuracy calculations [5] and support the previously predicted general spectral characteristics of the complex [6, 7]. The data obtained in this study are believed to be possibly of some help in the experimental search for the

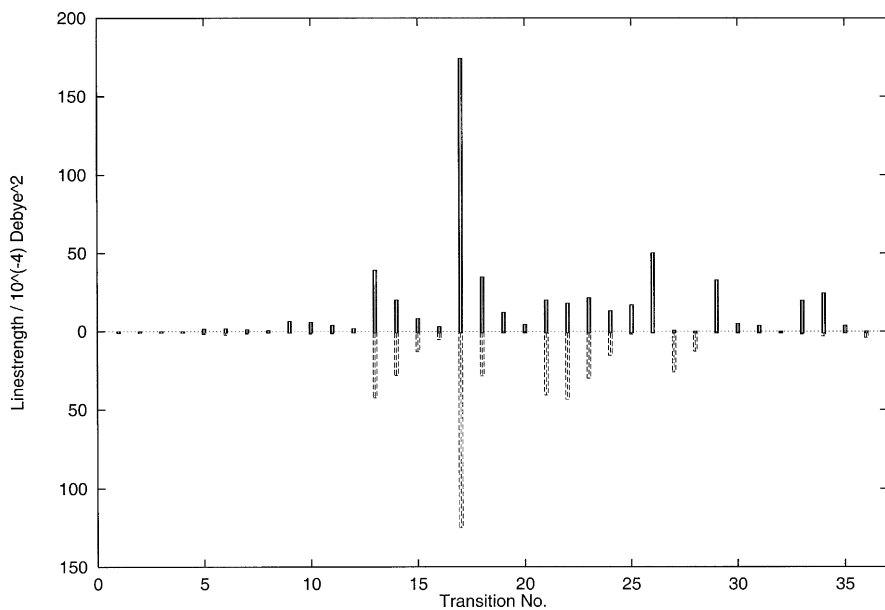


Fig. 2. Comparison of the linestrengths obtained from full-dimensional calculations (*solid lines* in the *upper part* of the plot) with the corresponding results from the Born-Oppenheimer approximation (*dashed lines* in the *lower part* of the plot) for transitions between the bound j -odd vibrational levels of the ground (\tilde{X}) and first excited (\tilde{A}) electronic states of HeH_2^+

still unobserved molecular spectra of the ion. They are certainly necessary when trying to evaluate theoretical rates for association or dissociation processes within one of the two electronic states, and even more importantly for a detailed state-to-state description of the radiative charge-transfer reaction of Eq. (1).

Acknowledgements. This work was supported by the Ministry of Education of the Czech Republic (project LN00A032). This study was completed when M.Š. and V.Š. were visiting the Max Planck Institute of Astrophysics. They are grateful for financial support and hospitality. W.P.K. gratefully acknowledges an invitation to visit the J. Heyrovský Institute of Physical Chemistry.

References

1. Abel T, Anninos P, Zhang Y, Norman ML (1997) *N. Astron.* 2: 181
2. Schauer MM, Jefferts SR, Barlow SE, Dunn GH (1989) *J Chem Phys* 91: 4593
3. Kraemer WP, Špirko V, Bludský O (2002) *Chem Phys* 276: 225
4. Falcetta MF, Siska PE (1999) *Mol Phys* 97: 117
5. Meuwly M, Hutson JM (1999) *J Chem Phys* 110: 3418
6. Juřek M, Špirko V, Kraemer WP (1997) *J Mol Spectrosc* 182: 364
7. Kraemer WP, Juřek M, Špirko V (1998) *J Mol Spectrosc* 187: 206
8. Špirko V, Kraemer WP (1995) *J Mol Spectrosc* 172: 265
9. Sutcliffe BT, Tennyson J (1986) *Mol Phys* 58: 1053
10. Johnson BR (1978) *J Chem Phys* 69: 4678